Original Article

Discovery and structural optimization of 4-(4-(benzyloxy)phenyl)-3,4-dihydropyrimidin-2(1H)-ones as RORc inverse agonists

Xi-shan WU[1, 2, #], Rui WANG[2, 3, #], Yan-li XING[2, 4, #], Xiao-qian XUE[2, 3], Yan ZHANG[2], Yong-zhi LU[2], Yu SONG[2, 4], Xiao-yu LUO[2], Chun WU[2], Yu-lai ZHOU[4], Jian-qin JIANG[1, *], Yong XU[2, *]

[1]Department of Natural Medicinal Chemistry, China Pharmaceutical University, Nanjing 211198, China; [2]Institute of Chemical Biology, Guangzhou Institutes of Biomedicine and Health, Chinese Academy of Sciences, Guangzhou 510530, China; [3]University of Chinese Academy of Sciences, Beijing 100049, China; [4]Department of Bioengineering, School of Pharmaceutical Sciences, Jilin University, Changchun 130021, China

Aim: Retinoic acid receptor-related orphan nuclear receptors (RORs) are orphan nuclear receptors that show constitutive activity in the absence of ligands. Among 3 subtypes of RORs, RORc is a promising therapeutic target for the treatment of Th17-mediated autoimmune diseases. Here, we report novel RORc inverse agonists discovered through structure-based drug design.
Methods: Based on the structure of compound **8**, a previously described agonist of RORa, a series of 4-(4-(benzyloxy)phenyl)-3,4-dihydropyrimidin-2(1H)-one derivatives were designed and synthesized. The interaction between the compounds and RORc was detected at molecular level using AlphaScreen assay. The compounds were further examined in 293T cells transfected with RORc and luciferase reporter gene. Thermal stability shift assay was used to evaluate the effects of the compounds on protein stability.
Results: A total of 27 derivatives were designed and synthesized. Among them, the compound **22b** was identified as the most potent RORc inverse agonist. Its IC_{50} values were 2.39 µmol/L in AlphaScreen assay, and 0.82 µmol/L in inhibition of the cell-based luciferase reporter activity. Furthermore, the compound **22b** displayed a 120-fold selectivity for RORc over other nuclear receptors. Moreover, a molecular docking study showed that the structure-activity relationship was consistent with the binding mode of compound **22b** in RORc.
Conclusion: 4-(4-(Benzyloxy)phenyl)-3,4-dihydropyrimidin-2(1H)-one derivatives are promising candidates for the treatment of Th17-mediated autoimmune diseases, such as rheumatoid arthritis, psoriasis, and multiple sclerosis.

Keywords: nuclear receptor; RORc; inverse agonist; SAR; structure-based optimization; autoimmune disease

Introduction

Nuclear receptors (NRs) are a large family of ligand-regulated transcription factors that control the expression of target genes involved in a range of physiological processes such as development, metabolism, and immunity[1]. The human NR superfamily is composed of 48 members. Approximately half of them have been characterized as ligand-activated transcription factors regulating the expression of target genes. The remaining receptors are considered to be orphan NRs because they do not have well-characterized ligands[2]. NRs share a

modular structure composed of an N-terminal domain (AF1), a DNA-binding domain (DBD), a hinge region, a ligand binding domain (LBD) and a transcriptional activation function domain 2 (AF2). Binding of ligands in the LBD results in the recruitment of transcriptional co-activators (*eg*, steroid receptor co-activator 1, SRC1), or co-repressors (*eg*, nuclear receptor co-repressor, NCoR)[3, 4].

Retinoic acid receptor-related orphan nuclear receptors (RORs) are examples of orphan nuclear receptors that show constitutive activity in the absence of ligands. There are three subtypes of RORs: RORα (NR1F1), RORβ (NR1F2) and RORγ (NR1F3), which are also known as RORa, b and c in humans[5]. The three RORs share a high degree of sequence similarity but display distinct tissue distribution patterns and distinct functional roles in the regulation of many physiological processes[6]. Two forms of RORγ are found in both humans

and mice, termed RORγ1 and RORγt; they only differ in their amino terminal domain. RORγ1 is expressed in a variety of tissues, including the thymus, muscle, kidney and liver, whereas RORγt (with a truncated N-terminus) is exclusively expressed in the cells of the immune system, eg, T helper cells and lymphoid tissue inducer cells[7, 8]. RORγt has been shown to have key functions in the differentiation of Th17 cells and the secretion of inflammatory cytokines such as interleukin 17 (IL-17)[9]. Recent studies indicate that the modulation of IL-17 levels in autoimmune diseases may be beneficial in treating diseases, including multiple sclerosis, psoriasis, rheumatoid arthritis and inflammatory bowel disease. Thus, RORc is a promising therapeutic target for the treatment of Th17-mediated autoimmune diseases[10, 11].

Since the discovery of the first small molecule T0901317 (1, Figure 1), many RORc ligands with agonistic and inverse agonistic activity have been disclosed in the literature[12, 13]. Some structurally complex natural products, such as digoxin (2) and ursolic acid (UA, 3), have been reported to be RORc inverse agonists[14-16]. Using the T0901317 scaffold as a lead compound, a series of synthetic RORc inverse agonists were developed, including SR1001 (4), SR1555 (5), and SR2211 (6)[17-19]. A team from Genentech identified N-isobutyl-N-((5-(4-(methylsulfonyl)phenyl)thiophen-2-yl)methyl)-1-phenylmethanesulfonamide as RORc inverse agonist (7, Figure 1) via a biochemical screening campaign[20]. Although the development of RORc inverse agonists has shown significant promise[21, 22], the development of new RORc selective modulators with therapeutic potential still remains an urgent need.

In this paper, we report the discovery of novel 4-(4-(benzyloxy)phenyl)-3,4-dihydropyrimidin-2(1H)-ones as potent RORc inverse agonists. Compound 8 has been previously described as an agonist of RORa[23]. Considering the sequence and structural similarity of RORa and RORc and their crucial role in the development of Th17-related diseases, compound

8 was assessed for its inhibitory effect on RORc. Compound 8 was identified using an AlphaScreen assay (IC$_{50}$=20.89 μmol/L). This result provided us with confidence that 8 was a genuine RORc inverse agonist. Thus, compound 8 was selected as the starting structure for further SAR study. Extensive optimization was conducted, which led to the discovery of a potent and selective RORc inverse agonist.

Materials and methods
General chemistry

All reagents were purchased from commercial sources and used without further purification. For the synthesized compounds described below, flash chromatography was performed using silica gel (300–400 mesh). All of the reactions were monitored by TLC using silica gel plates (fluorescence F254, UV light). ^{1}H NMR spectra were recorded on a Bruker AV-400 spectrometer (Bruker, Fallanden, Switzerland) at 400 or 500 MHz. ^{13}C NMR spectra were recorded at 400 or 500 MHz. CDCl$_{3}$ is deuterochloroform, and DMSO-d$_{6}$ is hexadeuterodimethylsulfoxide. All coupling constants were measured in hertz, and the chemical shifts (δ_H and δ_C) were quoted in parts per million (ppm) relative to TMS (δ 0), which was used as the internal standard. Abbreviations for NMR data are as follows: s=singlet, d=doublet, t=triplet, q=quartet, m=multiplet, dd=doublet of doublets, dt=doublet of triplets, app=apparent, and br=broad. The low or high resolution mass spectra (LRMS and HRMS) were measured on an Agilent 1200 HPLC-MSD mass spectrometer or an Applied Biosystems Q-STAR Elite ESI-LC-MS/MS mass spectrometer, respectively. The experimental procedures and characterization of all compounds are provided in the Supplementary information.

Biological assays
Protein and peptide preparation
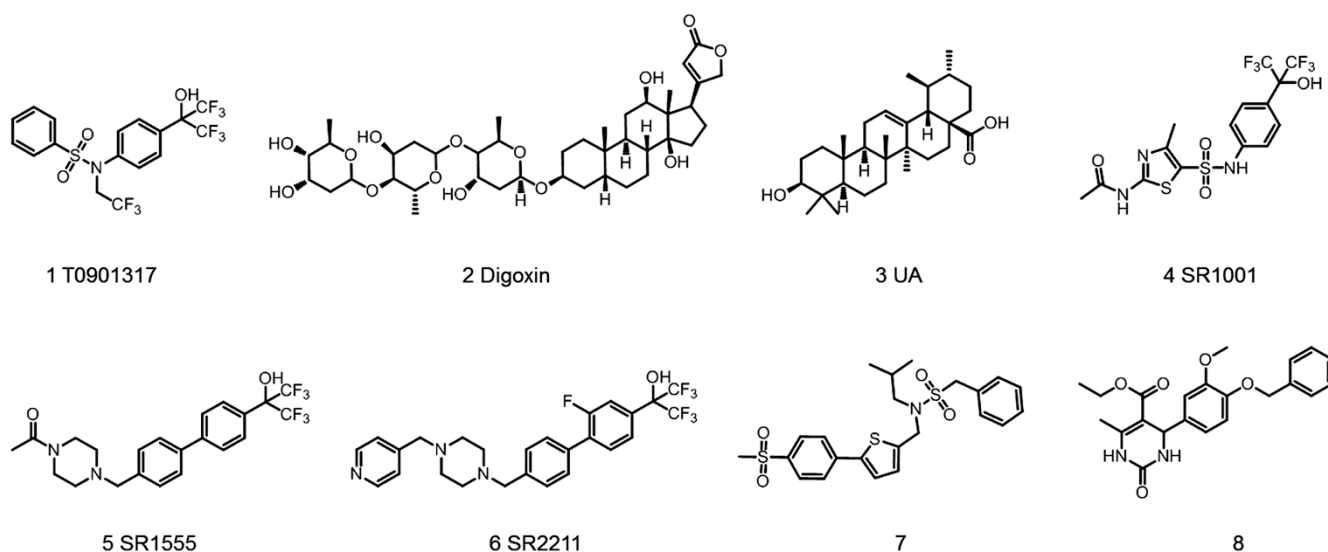The human RORc LBD (residues 262–507) was expressed as

Figure 1. Structures of RORc inverse agonists (1–7) and RORa agonist (8) from the literature.

a His6-fusion protein using the pET24a expression vector (Novagen, Madison, WI, USA)[24]. BL21 (DE3) cells that were transformed with this expression plasmid were grown in LB broth at 25 °C until an OD_{600} of approximately 1.0 was reached, and the cells were then induced with 0.1 mmol/L isopropyl-β-*D*-1-thiogalactopyranoside (IPTG) at 16 °C overnight. Cells were harvested, resuspended, and high-pressure homogenized in 200 mL of extract buffer (20 mmol/L Tris (pH 8.0), 500 mmol/L NaCl, 10% glycerol, and 25 mmol/L imidazole) per 6 L of cells. The lysate was centrifuged at 20 000 rounds per minute for 30 min, and the supernatant was loaded onto a 5-mL NiSO₄-loaded HisTrap HP column (GE Healthcare, Piscataway, NJ, USA). The column was washed with extract buffer, and the protein was eluted with a 25–500 mmol/L imidazole gradient. A gel filtration column (HiLoad S75, 16/60, GE Healthcare) was used for a second purification.

Transient transfection assays

Transient transfection assays were performed as described previously[11, 24]. 293T cells were maintained in DMEM containing 10% fetal bovine serum (FBS). Cells were transiently transfected in Opti-MEM using Lipofectamine 2000 (Invitrogen), according to the manufacturer's protocol. The 96-well plates were plated 24 h prior to transfection (15 000 cells per well). For all of the experiments, each well of cells was transfected in Opti-MEM with 25 ng of reporter plasmids and 5 ng of Renilla luciferase expression plasmids. For Gal4-driven reporter assays, the cells were transfected with 25 ng of Gal4-RORg LBD (residues 262–507) and 25 ng of pG5Luc reporter. For native promoter reporter assays, the cells were co-transfected with the Pcp2/RORE-Luc reporter along with the plasmids encoding full-length RORc. The cells were then transfected with the indicated expression and reporter plasmids. The media was changed 24 h after transfection, and the compounds were added. Cells were incubated for another 24 h followed by harvesting for a luciferase assay using the dual-luciferase reporter assay system (Promega). Luciferase data were normalized to Renilla luciferase data, which was used as an internal transfection control.

AlphaScreen assay

Interactions between RORc and ligands were assessed by luminescence-based AlphaScreen technology (Perkin Elmer) using a histidine detection kit from PerkinElmer (Norwalk, CT, USA) as previously described[24, 25]. All of the reactions contained 200 nmol/L receptor LBD bound to nickel acceptor beads (5 µg/mL) and 50 nmol/L biotinylated SRC1-4 peptide bound to streptavidin donor beads (5 µg/mL) in the presence or absence of the indicated concentration of control compound SR2211 or candidate compounds. The N-terminal biotinylated coactivator peptide SRC1-4 sequence was QKPTSGPQTPQA-QQKSLLQQLLTE. Compound concentrations varied from 150 nmol/L to 200 µmol/L in the dose-response assay.

Thermal stability shift assay

Thermal stability shift assay (TSA) is an increasingly popular method to identify small molecule ligands. In this study, TSA were carried out using the Bio-Rad CFX96 Real-Time PCR system. All reactions were buffered in 10 mmol/L HEPES, pH 7.5, 150 mmol/L NaCl and 5% (*v/v*) glycerol at a final concentration of 10 µmol/L protein and 200 µmol/L compounds. The 20 µL reaction mix was added to the wells of 96-well PCR plates. SYPRO Orange (ABI, Sigma) was added as a fluorescence probe at a dilution of 1:1000 and incubated with compounds on ice at least 30 min. Total DMSO concentration was restricted to 2% or less. The temperature was raised with a step of 0.5 °C per minute from 30 °C to 80 °C, and fluorescence readings were taken at each (0.5 °C) interval. All experiments were performed in triplicates for the RORc inverse agonist screen. Melting temperatures (T_m) were calculated by fitting the sigmoidal melt curve to the Boltzmann equation using GraphPad Prism. ΔT_m is the difference in T_m values calculated for reactions with and without compounds[26, 27].

Molecular docking simulation

The crystal structure of RORc in complex with compound **7** (PDB code: 4QM0) was used as the reference structure in the docking study. Protein structure preparation for docking studies included water deletion, hydrogen atom addition and protonation state adjustment. All of the ligand and protein preparations were performed in Maestro (version 9.4, Schrödinger, LLC, New York, NY, USA. 2013), implemented in the Schrödinger program (http://www.schrodinger.com). The Glide docking program with SP score was used for binding mode prediction[28].

Results
Design rationality

In this study, we try to develop new RORc inverse agonists starting from compound **8** which was identified as RORa agonist[23]. In order to predict RORc-**8** binding modes, we analyzed known RORc-ligand complex structures. In a previous study from Genentech, compound **7** (Figure 1) was demonstrated to be a potent RORc inverse agonist. In the RORc-LBD-**7** complex structure (PDB code: 4QM0), the benzylic ring of **7** formed a π–π interaction with His479 and disturbed the secondary structure for helices 11'–12 in the RORc-LBD co-structure, which may account for the RORc inverse agonist profile of **7**. The N-isobutyl group of **7** resided in a shallow hydrophobic pocket lined with Val376, Phe388, and Phe401. It is worth noting that access to the shallow hydrophobic pocket may help to achieve potency improvement[20].

Because there is an asymmetric center in this scaffold, we first investigated the differences in the RORc binding modes of the S and R configurations of **8**. The molecular docking result showed that the (S) enantiomer had a repeatable and stable binding mode. Thus, we selected **8** (S) for a docking study, and all further docking studies were carried out with **8** (S). In the following discussion, we explored the SAR of this series, with a concentration on the right-hand side of the molecule, which does not involve the asymmetric center. Therefore, compounds were synthesized as racemates to rapidly produce

structure-activity data.

The molecular docking study of **8** (S) (Figure 2A) and **8** (S) overlaid with **7** (Figure 2B) was performed. In compound **8**, the carbonyl oxygen of the urea and ester moiety interacted with the amino acid residues Gly380 and Gln286 through H-bonds. Two π-π interactions exist between compound **8** and His323 and Phe388. Upon careful examination of the binding mode of **8** (S) overlaid with **7**, we considered the effects of increasing the size of the terminal aromatic ring of **8** by introducing substituents that would interfere with the packing of helix12. In addition, we also considered the effects of introducing substituents on the terminal aryl ring of **8** to access the hydrophobic pocket lined with Val376, Phe388, and Phe401. We investigated whether this modification (Figure 3) on the terminal aryl ring of **8** could improve the activity of RORc.

Synthesis

Compounds **15a-l** and **18a-l** were synthesized as shown in Scheme 1. The key intermediates **12a-c** were synthesized from 4-hydroxybenzaldehyde (**9a-c**), urea (**10**) and ethyl acetoacetate (**11**) with anhydrous $ZnCl_2$ by means of a Biginelli multicomponent reaction[23]. Compounds **13a-l** and **16a-l** were reduced with $NaBH_4$ in the presence of ethanol, followed by treatment with phosphorus tribromide in DMF, which generated intermediates **14a-l** and **17a-l**, respectively. Condensation of intermediates **14a-l** and **17a-l** with intermediates **12a-b** was accomplished using the Williamson ether synthesis to afford the desired target compounds **15a-l** and **18a-l**[29].

Compounds **22a** and **22b** were synthesized as shown in Scheme 2. Compounds **19a-b** were reacted with phenol by using the Williamson ether synthesis in the presence of Cs_2CO_3 to give intermediates **20a-b**. Compounds **20a-b** were reduced with $NaBH_4$, followed by treatment with phosphorus tribromide, which resulted in intermediates **21a-b**. Condensation of the obtained intermediates **21a-b** with the intermediate **12b** was accomplished using the Williamson ether synthesis to afford the desired target compounds **22a** and **22b**.
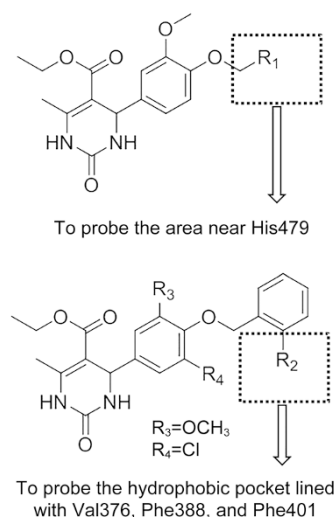

To probe the area near His479

To probe the hydrophobic pocket lined with Val376, Phe388, and Phe401

$R_3=OCH_3$
$R_4=Cl$

Figure 3. Strategy for structural optimization.

SAR analysis

We first explored the introduction of additional steric bulk on the terminal aryl ring of **8** in an effort to interfere with the packing of helix12. As demonstrated in Table 1, the introduction of a fluorine atom (**15a**) at the 4-position of the terminal phenyl ring of **8** resulted in a significant loss of potency. Naphthalene (**15b**) and quinoxaline (**15c**) derivatives also resulted in a complete loss of activity, whereas benzodioxole (**15d**) derivatives showed better activity than **8**. To further investigate the impact of introducing larger substituents onto the terminal aromatic ring, compound **15e** was synthesized. However, compound **15e** had no activity. Replacement of the phenyl ring in compound **15e** with a thiophene (**15f**) resulted in a slight potency decrease compared to **8**. Interestingly, inserting an oxygen atom between biphenyl groups at the R_1 position dramatically improved RORc inhibition (**15g**, **15h**, **15i** *vs* **15e**). Compound **15g** (IC_{50}=3.47 μmol/L)
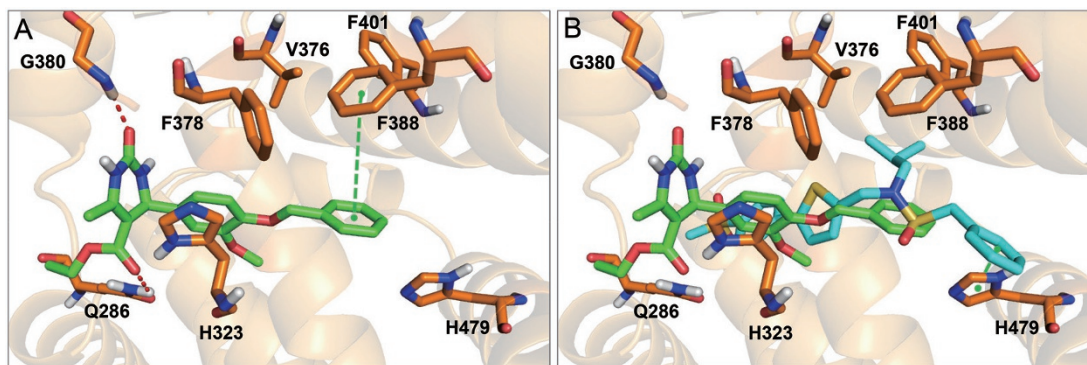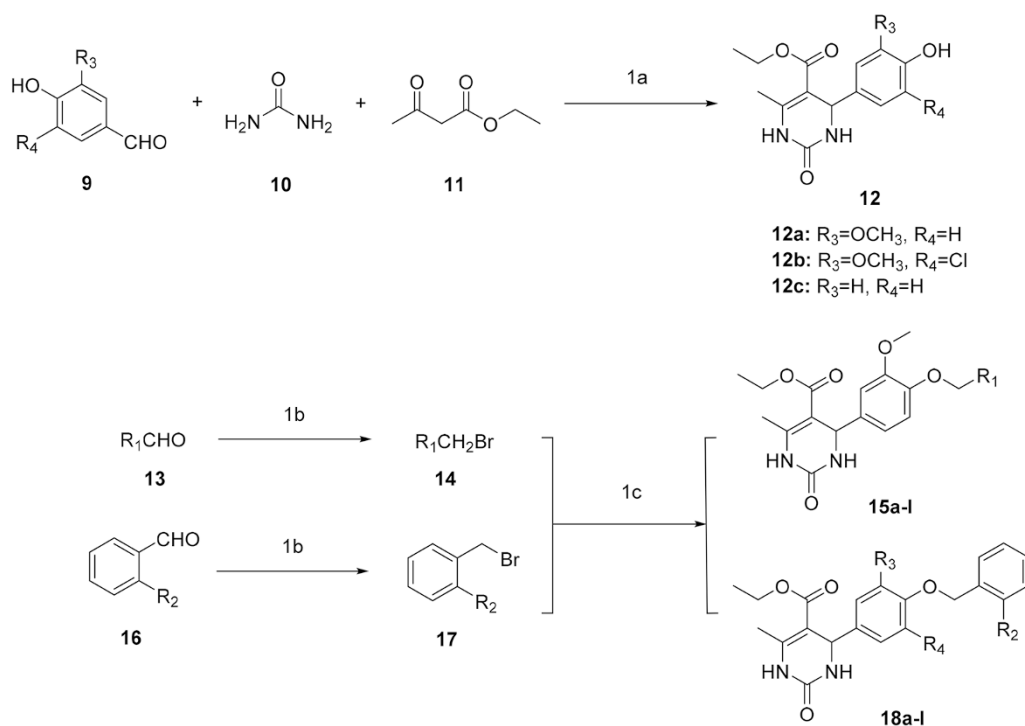

Figure 2. Predicted binding modes of ligands with RORc. (A) The docking models of compound **8** (green) in the RORc ligand binding pocket (orange). (B) The superimposition of the binding modes of **7** (cyan) and **8** (green). The ligands and important residues are shown as sticks. Hydrogen bonds are depicted as red dashed lines, and π–π interactions indicted by green dashed lines.

Scheme 1. Reagents and conditions: (1a) ZnCl$_2$, 80 °C, 1 h; (1b) 1. NaBH$_4$, EtOH, rt, 1 h; 2. PBr$_3$, DCM, rt, 1 h; (1c) **12**, K$_2$CO$_3$, DMF, 80 °C, 4 h.
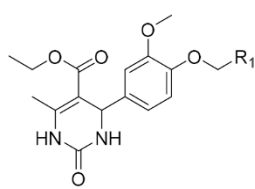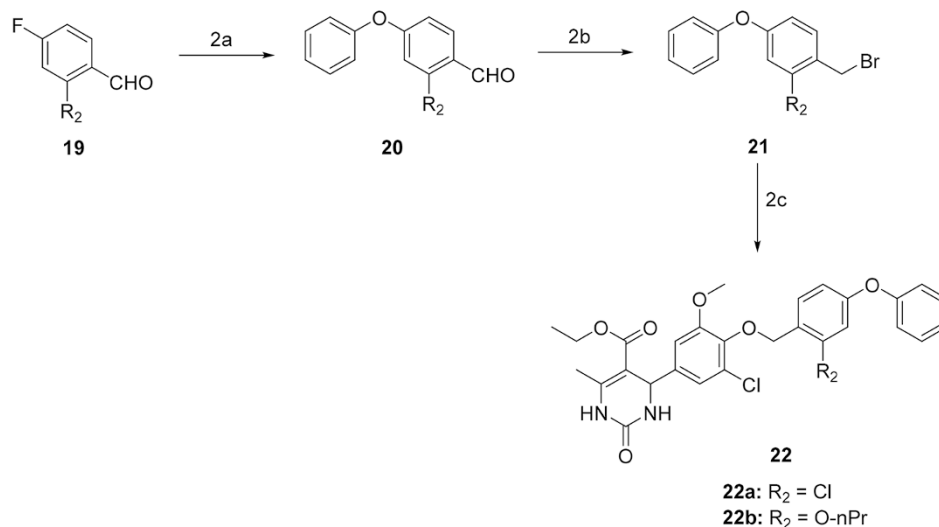

Scheme 2. Reagents and conditions: (2a) phenol, Cs$_2$CO$_3$, DMF, 75 °C, 4 h; (2b) 1. NaBH$_4$, EtOH, rt, 1 h; 2. PBr$_3$, DCM, rt, 1 h; (2c) **12b**, K$_2$CO$_3$, DMF, 80 °C, 4 h.

demonstrated a 6-fold improved inhibition compared with **8** (IC$_{50}$=20.89 μmol/L), whereas adding one flexible carbon atom between the oxygen atom and the terminal aryl ring led to a slight reduction in RORc potency (**15j** *vs* **15g**). These results indicated that the presence of two aromatic rings linked with a flexible atom, such as an oxygen atom, at the R$_1$ position increases the potency of the compounds, which is presumably due to the π-π stacking interaction between the terminal aryl

ring of the compounds (**15g**, **15h**, **15i**) and His479 residues, which interfere with the packing of helix12 in the AF2 region. We further synthesized compounds **15k** and **15l**. The results demonstrated that both compounds resulted in a complete loss of activity.

We next investigated the modification of substituent R$_2$ (Table 2) to probe the hydrophobic pocket lined with Val376, Phe388, and Phe401. Taking into account the synthetic chal-
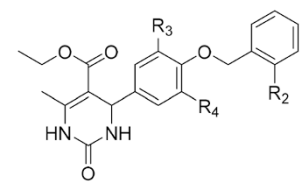
Table 1. SAR at the R_1 position.

Compound	R_1	AlphaScreen IC$_{50}$ (µmol/L)[a] (% max inhibition)	TSA ΔT_m (°C)[b]
8		20.89±0.68 (99)	NA
15a		NA	NA
15b		NA	1.9
15c		NA	NA
15d		8.71±1.33 (87)	4.0
15e		NA	NA
15f		29.38±5.81 (65)	4.0
15g		3.47±0.07 (75)	3.4
15h		5.99±1.12 (55)	2.7
15i		6.32±0.70 (63)	NA
15j		7.37±0.16 (73)	3.1
15k		NA	NA
15l		NA	NA

All assay results are reported as the arithmetic mean±SD from at least two independent experiments, NA=not active.

[a] Inhibition of RORc LBD recruitment of the biotin-SRC1–4 co-activator peptide.

[b] Inhibition of TSA activity of RORc by tested compounds.

Table 2. SAR at the R_2, R_3, and R_4 positions.

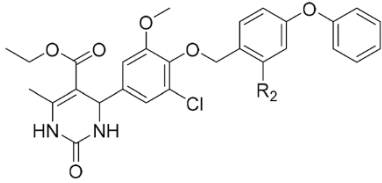| Compound	R_2	R_3	R_4	AlphaScreen IC$_{50}$ (µmol/L)[a] (% max inhibition)	TSA ΔT_m (°C)[b]
18a	H	H	H	NA	NA
18b	Cl	OCH$_3$	H	21.24±1.22 (67)	5.2
18c	CH$_3$	OCH$_3$	H	NA	4.9
18d	OCH$_3$	OCH$_3$	H	NA	6.9
18e	OC$_2$H$_5$	OCH$_3$	H	NA	4.5
18f	O-nPr	OCH$_3$	H	6.38±0.38 (69)	5.8
18g	O-nBu	OCH$_3$	H	8.86±2.85 (65)	5.2
18h	OBn	OCH$_3$	H	8.87±0.24 (86)	4.7
18i	Cl	OCH$_3$	Cl	4.72±0.06 (89)	6.4
18j	O-nPr	OCH$_3$	Cl	5.51±0.75 (67)	7.3
18k	O-nBu	OCH$_3$	Cl	4.74±0.25 (91)	7.5
18l	OBn	OCH$_3$	Cl	5.10±0.95 (87)	7.0

All assay results are reported as the arithmetic mean±SD from at least two independent experiments, NA=not active.

[a] Inhibition of RORc LBD recruitment of the biotin-SRC1–4 co-activator peptide.

[b] Inhibition of TSA activity of RORc by tested compounds.

lenges, we also selected **8** as the starting point for further structural optimization. We first examined the importance of the methoxy substitution at the R_3 position. When comparing compounds **18a** and **8**, it appeared that methoxy substitution at the R_3 position favored efficacy. We then explored a range of substituents at the R_2 position (Table 2). With the methoxy group maintained at the R_3 position, R_2 was modified from H to halogen, small alkyls, and small alkoxyl groups. The results of these modifications showed that the small substituents at the R_2 position did not provide any potency improvement (**18b**, **18c**, **18d**, **18e** *vs* **8**). In the R_2 position, substituents with different groups that were linked by an oxygen atom were attached to the aryl ring as a means of probing the intended cavity. Compounds **18f** (O-nPr), **18g** (O-nBu) and **18h** (OBn) were synthesized and exhibited improved activity. Compound **18f** exhibited the best activity, with an IC$_{50}$ of 6.38 µmol/L and a temperature shift of 5.8 °C in the thermal shift assay. This result indicated that the propoxy group at the R_2 position is the optimal size and fits very well in the hydrophobic pocket. Additionally, when comparing compounds **18b**, **18f**, **18g** and **18h** with compounds **18i**, **18j**, **18k** and **18l**, respectively, it appeared that the introduction of a chlorine atom at the R_4 position increased RORc potency.

Finally, all the beneficial changes were combined, and compounds **22a** and **22b** were designed and synthesized (Table 3).

Table 3. SAR at the R_2 position.

Compound	R_2	AlphaScreen IC$_{50}$ (µmol/L)[a] (% max inhibition)	Luciferase IC$_{50}$ (µmol/L)[b] (% max inhibition)	TSA ΔT_m (°C)[c]
22a	Cl	4.60±0.35 (92)	2.84±0.42	4.9
22b	O-nPr	2.39±0.11 (98)	0.82±0.00 (93)	5.2

All assay results are reported as the arithmetic mean±SD from at least two independent experiments, NA=not active.
[a] Inhibition of RORc LBD recruitment of the biotin-SRC1–4 co-activator peptide.
[b] Inhibition of Luciferase reporter activity of RORc by tested compounds.
[c] Inhibition of TSA activity of RORc by tested compounds.

Furthermore, we also evaluated their cell activity in a reporter gene assay. As expected, both compounds showed good RORc inhibition activity. Compound **22b** was the most potent RORc inverse agonist among all the compounds. The IC$_{50}$ of **22b** was 2.39 µmol/L and 0.82 µmol/L in the protein-based AlphaScreen assay and the reporter gene assay, respectively (Figure 4). The TSA assay also showed a stabilizing effect on the RORc protein with a temperature shift of 5.2 °C.

Selectivity profile

To assess the selectivity profile for the three isoforms of ROR, we profiled the potent inverse agonist compounds with 293T cell-based assays using Gal4-NR constructs (Table 4). In addition, the selectivity profiles of these compounds for the farnesoid X receptor (FXR) and liver X receptor (LXR)-α were investigated using the same cell-based luciferase reporter gene assay[30].
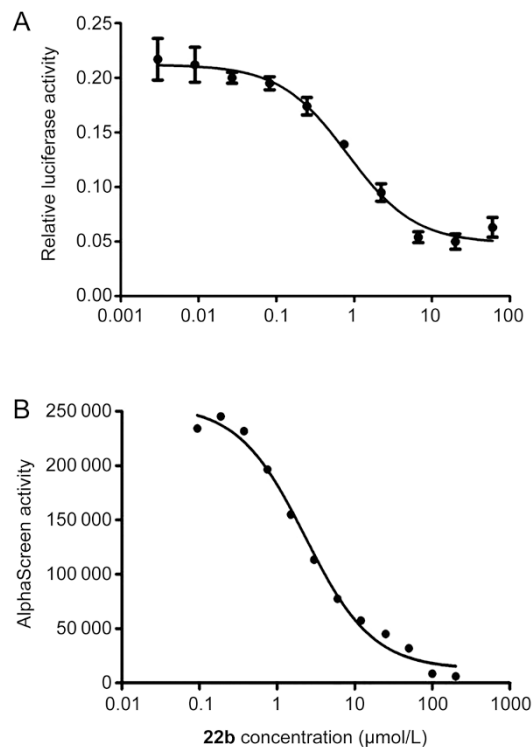
Compounds **15g**, **18f**, **18k**, **18l** and **22b** exhibited potent RORc activity in the reporter gene assay and excellent selec-
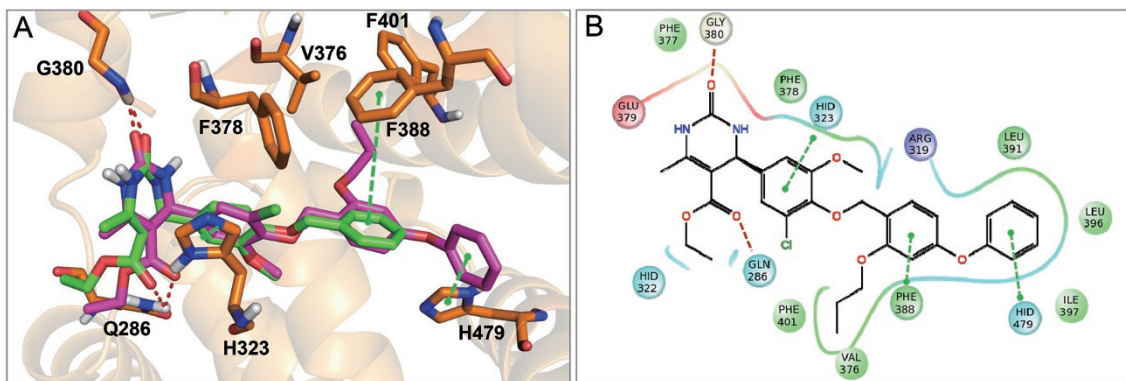

Figure 4. Dose-response curves for suppression of the derivative activity of RORc by **22b** in the Dual Luciferase assay (A) and AlphaScreen assay (B). The IC$_{50}$ values are 2.39 and 0.82 µmol/L, respectively.

tivity for RORc versus the other NRs in our selectivity panel. One highlight from this work was that **22b** was the most potent RORc inverse agonist, with more than a 120-fold selectivity over the other NRs. **22b** showed weak activity at FXR and LXRα. The results indicated that **22b** gave a significantly improved selectivity window over the other NRs.

Discussion

To rationalize the SAR between these novel inverse agonists and RORc, a molecular docking study was performed with the most potent compound **22b** (S) (Figure 5). The binding model of **22b** (S) (Figure 5A) was similar to that of **8** (S) (Fig-

Table 4. RORc potency and selectivity profiles in Gal4 human transcription assays[a].

Cmpd	Gal4-RORγ-LBD	Gal4-RORα-LBD	Gal4-RORβ-LBD	Gal4-LXRα-LBD	Gal4-FXR-LBD
15g	1.22±0.06 (91)	>100 (44)	>100 (26)	>100 (33)	>100 (13)
18f	0.39±0.00 (95)	>100 (49)	>100 (8)	>100 (15)	>100 (6)
18k	1.06±0.06 (81)	>100 (22)	>100 (13)	>100 (5)	>100 (10)
18l	0.99±0.12 (89)	>100 (27)	>100 (9)	>100 (6)	>100 (8)
22b	0.82±0.00 (93)	>100 (19)	>100 (5)	>100 (7)	>100 (8)

All assay results are reported as the arithmetic mean±SD from at least two independent experiments.
[a] All assays were conducted in 293T cells transiently transfected with Gal4-NR-LBD luciferase plasmids. All NR assays monitored the suppression of their respective basal transcriptional activities, an outcome consistent with the inverse agonist activity of the ligands. In this table, positive % max indicates suppression of the basal reporter signal relative to DMSO-treated cells.

Figure 5. Predicted binding modes of ligands with the RORc protein. (A) 3D presentation of the predicted binding mode of **22b** (magenta) superimposed with **8** (green) in the ligand binding pocket. (B) 2D schematic presentation of the predicted binding mode of **22b** in the ligand binding pocket. The ligands and important residues are shown as sticks. Hydrogen bonds are depicted as red dashed lines, and π-π interactions indicted by green dashed lines.

ure 2A). For compound **22b**, the carbonyl oxygen of the urea and ester moiety form two hydrogen bonds with the backbone of Gly380 and Gln286. Three π-π interactions exist between compound **22b** and His323, Phe388 and His479. The propoxy group of compound **22b** resided in a shallow lipophilic pocket lined with Val376, Phe388 and Phe401. Docking results demonstrated that the SAR was consistent with the binding mode of compound **22b**. Therefore, the docking simulations further confirmed that **22b** is a favorable RORc inverse agonist. As discussed above, we showed that two aromatic rings linked with a flexible atom at the R_1 position were crucial for RORc inhibition and that the size of the substituent at the R_2 position was correlated with potency. These findings provide an important structural basis for further ligand optimization and suggest that inverse agonists for RORc with even higher pharmacological utility can be obtained in the near future.

In summary, we designed and optimized a new series of RORc inverse agonists comprising a 4-(4-(benzyloxy)phenyl)-3,4-dihydropyrimidin-2(1H)-one scaffold. A total of 27 target compounds were synthesized and evaluated for their inhibitory activity against RORc. Compound **22b** was the most potent RORc inverse agonist in this series and displayed more than a 120-fold selectivity for RORc over other NRs as assessed by cellular assays. It is notable that **22b** lacked inhibitory activity for RORa. The most potent and selective compound may serve as a useful tool for developing RORc inverse agonists. Further structural optimization and *in vivo* studies are currently in progress and will be reported in due course.

Acknowledgements

Author contribution

Yong XU, Jian-qin JIANG, and Yu-lai Zhou designed the experiments; Xi-shan WU, Rui WANG, and Yan-li XING, performed the experiments. All authors participated in data acquisition, analysis, and interpretation. Xi-shan WU, Rui WANG, Yan-li XING, Xiao-qian XUE, Yan ZHANG, and Yong XU wrote the paper. All authors reviewed the final manuscript.

Supplementary information

Supplementary information is available at the Acta Pharmacologica Sinica's website.

References

1 Kamenecka TM, Lyda B, Chang MR, Griffin PR. Synthetic modulators of the retinoic acid receptor-related orphan receptors. Med Chem Comm 2013; 4: 764–76.
2 Toyama H, Nakamura M, Nakamura M, Matsumoto Y, Nakagomi M, Hashimoto Y. Development of novel silicon-containing inverse agonists of retinoic acid receptor-related orphan receptors. Bioorg Med Chem 2014; 22: 1948–59.
3 Wang Y, Cai W, Zhang G, Yang T, Liu Q, Cheng Y, *et al*. Discovery of novel N-(5-(arylcarbonyl)thiazol-2-yl)amides and N-(5-(arylcarbonyl) thiophen-2-yl)amides as potent RORgammat inhibitors. Bioorg Med Chem 2014; 22: 692–702.
4 Jetten AM, Ueda E. Retinoid-related orphan receptors (RORs): roles in cell survival, differentiation and disease. Cell Death Differ 2002; 9: 1167–71.
5 Gege C, Schluter T, Hoffmann T. Identification of the first inverse agonist of retinoid-related orphan receptor (ROR) with dual selectivity for RORbeta and RORgammat. Bioorg Med Chem Lett 2014; 24: 5265–7.

6 Chao J, Enyedy I, Van Vloten K, Marcotte D, Guertin K, Hutchings R, *et al*. Discovery of biaryl carboxylamides as potent RORgamma inverse agonists. Bioorg Med Chem Lett 2015; 25: 2991–7.

7 Ranhotra HS. The interplay between retinoic acid receptor-related orphan receptors and human diseases. J Recept Signal Transduct Res 2012; 32: 181–9.

8 Solt LA, Griffin PR, Burris TP. Ligand regulation of retinoic acid receptor-related orphan receptors: implications for development of novel therapeutics. Curr Opin Lipidol 2010; 21: 204–11.

9 Khan PM, El-Gendy Bel D, Kumar N, Garcia-Ordonez R, Lin L, Ruiz CH, *et al*. Small molecule amides as potent ROR-gamma selective modulators. Bioorg Med Chem Lett 2013; 23: 532–6.

10 Ouyang W, Kolls JK, Zheng Y. The biological functions of T helper 17 cell effector cytokines in inflammation. Immunity 2008; 28: 454–67.

11 Zhang Y, Xue X, Jin X, Song Y, Li J, Luo X, *et al*. Discovery of 2-oxo-1,2-dihydrobenzo[cd]indole-6-sulfonamide derivatives as new RORgamma inhibitors using virtual screening, synthesis and biological evaluation. Eur J Med Chem 2014; 78: 431–41.

12 Fauber BP, Magnuson S. Modulators of the nuclear receptor retinoic acid receptor-related orphan receptor-gamma (RORgamma or RORc). J Med Chem 2014; 57: 5871–92.

13 Huh JR, Littman DR. Small molecule inhibitors of RORgammat: targeting Th17 cells and other applications. Eur J Immunol 2012; 42: 2232–7.

14 Fujita-Sato S, Ito S, Isobe T, Ohyama T, Wakabayashi K, Morishita K, *et al*. Structural basis of digoxin that antagonizes RORgamma t receptor activity and suppresses Th17 cell differentiation and interleukin (IL)-17 production. J Biol Chem 2011; 286: 31409–17.

15 Huh JR, Leung MW, Huang P, Ryan DA, Krout MR, Malapaka RR, *et al*. Digoxin and its derivatives suppress TH17 cell differentiation by antagonizing RORgammat activity. Nature 2011; 472: 486–90.

16 Xu T, Wang X, Zhong B, Nurieva RI, Ding S, Dong C. Ursolic acid suppresses interleukin-17 (IL-17) production by selectively antagonizing the function of RORgamma t protein. J Biol Chem 2011; 286: 22707–10.

17 Kumar N, Lyda B, Chang MR, Lauer JL, Solt LA, Burris TP, *et al*. Identification of SR2211: a potent synthetic RORgamma-selective modulator. ACS Chem Biol 2012; 7: 672–7.

18 Solt LA, Kumar N, He Y, Kamenecka TM, Griffin PR, Burris TP. Identification of a selective RORgamma ligand that suppresses T(H)17 cells and stimulates T regulatory cells. ACS Chem Biol 2012; 7: 1515–9.

19 Solt LA, Kumar N, Nuhant P, Wang Y, Lauer JL, Liu J, *et al*. Suppression of TH17 differentiation and autoimmunity by a synthetic ROR ligand. Nature 2011; 472: 491–4.

20 Fauber BP, Rene O, de Leon Boenig G, Burton B, Deng Y, Eidenschenk C, *et al*. Reduction in lipophilicity improved the solubility, plasma-protein binding, and permeability of tertiary sulfonamide RORc inverse agonists. Bioorg Med Chem Lett 2014; 24: 3891–7.

21 Fauber BP, de Leon Boenig G, Burton B, Eidenschenk C, Everett C, Gobbi A, *et al*. Structure-based design of substituted hexafluoroisopropanol-arylsulfonamides as modulators of RORc. Bioorg Med Chem Lett 2013; 23: 6604–9.

22 Yang T, Liu Q, Cheng Y, Cai W, Ma Y, Yang L, *et al*. Discovery of tertiary amine and indole derivatives as potent RORgammat inverse agonists. ACS Med Chem Lett 2014; 5: 65–8.

23 Dubernet M, Duguet N, Colliandre L, Berini C, Helleboid S, Bourotte M, *et al*. Identification of new nonsteroidal RORalpha ligands; related structure-activity relationships and docking studies. ACS Med Chem Lett 2013; 4: 504–8.

24 Jin L, Martynowski D, Zheng S, Wada T, Xie W, Li Y. Structural basis for hydroxycholesterols as natural ligands of orphan nuclear receptor RORgamma. Mol Endocrinol 2010; 24: 923–9.

25 Suino-Powell K, Xu Y, Zhang C, Tao YG, Tolbert WD, Simons SS Jr, *et al*. Doubling the size of the glucocorticoid receptor ligand binding pocket by deacylcortivazol. Mol Cell Biol 2008; 28: 1915–23.

26 Niesen FH, Berglund H, Vedadi M. The use of differential scanning fluorimetry to detect ligand interactions that promote protein stability. Nat Protoc 2007; 2: 2212–21.

27 Pantoliano MW, Petrella EC, Kwasnoski JD, Lobanov VS, Myslik J, Graf E, *et al*. High-density miniaturized thermal shift assays as a general strategy for drug discovery. J Biomol Screen 2001; 6: 429–40.

28 Friesner RA, Banks JL, Murphy RB, Halgren TA, Klicic JJ, Mainz DT, *et al*. Glide: a new approach for rapid, accurate docking and scoring. 1. Method and assessment of docking accuracy. J Med Chem 2004; 47: 1739–49.

29 Li Z, Wang X, Xu X, Yang J, Xia W, Zhou X, *et al*. Design, synthesis and biological activity of phenoxyacetic acid derivatives as novel free fatty acid receptor 1 agonists. Bioorg Med Chem 2015; 23: 7158–64.

30 van Niel MB, Fauber BP, Cartwright M, Gaines S, Killen JC, Rene O, *et al*. A reversed sulfonamide series of selective RORc inverse agonists. Bioorg Med Chem Lett 2014; 24: 5769–76.